Supramolecular Architecture and Magnetic Properties of Copper(II) and Nickel(II) Porphyrinogen – TCNQ Electron-Transfer Salts

Loreto Ballester,[a] Ana M. Gil,[a] Angel Gutiérrez,*[a] M. Felisa Perpiñán,[a] M. Teresa Azcondo,[b] Ana E. Sánchez,[b] Claude Marzin,[c] Georges Tarrago,[c] and Carlo Bellitto[d]

Abstract: The compounds [Cu(Tz)-(MeOH)$_2$](TCNQ)$_2$ (**1**), [Ni(Tz)-(MeOH)$_2$](TCNQ)$_2$ (**2**), [Cu(Tz)$_2$]-(TCNQ)$_7$ (**3**) and [Ni(Tz)$_2$](TCNQ)$_7$ (**4**) (Tz = 2,7,12,17-tetramethyl-1,6,11,16-tetraazaporphyrinogen) were obtained by metathesis reaction of [M(Tz)](ClO$_4$)$_2$ with LiTCNQ and Et$_3$NH(TCNQ)$_2$, respectively. They were characterized by a combination of spectroscopic and physical methods. Compound **1** crystallizes in the monoclinic space group $P2_1/n$ with $a = 8.310(2)$, $b = 25.180(4)$, $c = 20.727(4)$ Å, $\beta = 93.58(2)°$; $Z = 4$. Compound **3** crystallizes in the triclinic space group P$\bar{1}$ with $a = 11.244(1)$, $b = 16.700(1)$, $c = 17.321(1)$ Å, $\alpha = 113.47(1)$, $\beta = 108.52(1)$, $\gamma = 96.12(1)°$; $Z = 2$. The asymmetric unit of the compound **1** is formed by cationic [Cu(Tz)(MeOH)$_2$]$^{2+}$ and by two crystallographically non equivalent TCNQ$^{•-}$

anions; these anions form dimeric units by overlap of the π clouds. The dimers form hydrogen bonds with the metallomacrocyclic cation through the methanol ligands. According to this structure the compound is paramagnetic and behaves as an insulator in the temperature range studied. The paramagnetism arises only from the metal-complex moieties. Compound **3** shows an unprecedented structure due to the steric requirements of the macrocycle that favors the stacking of the TCNQ groups. The structure consists of infinite stacks of TCNQ units separated by the metal-macrocyclic units; there are seven

TCNQ molecules per formula unit, one of which is formally mono-anionic, while the other six bear one half of an electron per molecule. The copper is six-coordinate in a very distorted octahedral environment. The Tz ligand is located in the equatorial plane and the apical nitrogens of the nitrile groups of two TCNQ molecules complete the coordination around the copper. The compound is a semiconductor and its magnetic behavior can be explained by the sum of the Curie contribution of the metal complex and the contribution arising from the magnetic-exchange interactions of the spins located on the TCNQ units. The latter is found to be typical of one-dimensional antiferromagnetic distorted chains of S = ½ spins and can be fitted according to a one-dimensional Heisenberg antiferromagnetic model.

Introduction

Much effort has been devoted to the study of the correlation between supramolecular architecture and properties in donor-

[a] Dr. A. Gutiérrez, Prof. Dr. L. Ballester, A. M. Gil, Dr. M. F. Perpiñán
Departamento de Química Inorgánica
Facultad de Ciencias Químicas
Universidad Complutense, 28040 Madrid (Spain)
Fax: (+34) 913-944-352
E-mail: alonso@quim.ucm.es

[b] Dr. M. T. Azcondo, Dr. A. E. Sánchez
Departamento de Química Inorgánica y Materiales
Facultad de Ciencias Experimentales y Técnicas
Universidad San Pablo-CEU (Spain)

[c] Dr. C. Marzin, Dr. G. Tarrago
Equipe de Chimie Supramoléculaire
Laboratoire des Matériaux et Procédés Membranaires
LMPM UMR 9987, Université Montpellier II/CNRS (France)

[d] Dr. C. Bellitto
Istituto di Chimica dei Materiali del C.N.R.
00016 Monterotondo Staz., Roma (Italy)

acceptor systems in which both units are organic molecules.[1] On the other hand, new behavior is expected when paramagnetic transition metal centers are introduced as building blocks in these supramolecular arrays.[2]

One of the most widely used organic planar acceptors in the synthesis of electrically conductive molecule-based materials is the TCNQ molecule (7,7,8,8-tetracyanoquinodimethane). In combination with a metallic fragment, the metal has proved to influence greatly the orientation of the TCNQ units in the stack, since in its reduced form the radical anion [TCNQ$^{•-}$], tends to coordinate the transition metals through one of the nitrogen atoms of the nitrile groups.[3] A common feature found in these compounds is the presence of the dimeric dianion [TCNQ]$_2$$^{2-}$ formed by the overlap of the π-electron clouds of adjacent radical anions.[4]

We have recently studied the influence of tetraazamacrocyclic complexes of nickel(II) and copper(II) on the electronic and magnetic properties of M^{II}(macrocyclic) – TCNQ systems and four different kinds of supramolecular architectures have

been observed, depending on the TCNQ oxidation states and the ability to form σ metal–TCNQ bonds.

If the reaction is carried out in the presence of only the anionic [TCNQ]⁻, and the metal complex has labile ligands or vacant coordinative positions, then the compounds obtained contain [TCNQ]⁻ anions bonded to the metal in a monodentate fashion. The coordinated anion-radicals are dimerized, leading to the formation of infinite chains with these [TCNQ]₂²⁻ dimers bridging consecutive metallic fragments.[4] However, when the metal ion has a close stable coordinative environment, thus precluding a direct interaction with the anion radical, the crystal packing is driven by electrostatic interactions between the cationic metal moieties and the dimeric [TCNQ]₂²⁻ anions which alternate in the solid.[4d, 5]

If the reaction is carried out in the presence of the mixed valence (Et₃NH)[TCNQ]₂, two new supramolecular architectures have been observed. In the first case, if the radical anion can coordinate the metal atom, the previously mentioned chains $\cdots$ −[M(N₄)]−(TCNQ)₂−[M(N₄)]−(TCNQ)₂−$\cdots$ are formed. The difference comes from the presence of neutral TCNQ molecules, which connect adjacent chains by overlap with the clouds of the coordinated TCNQ anions. These neutral molecules thus extend the interactions to a second direction in the crystal structure.[6] Finally, if no direct interaction with the metal is present, the TCNQ units show a greater electronic delocalization, with stacks made of formally [TCNQ]⁰·⁵⁻ or [TCNQ]⁰·⁶⁶⁻ separated by rows of the cationic metal complexes.[7]

With the aim of obtaining novel supramolecular architectures, the macrocycle, 2,7,12,17-tetrametyl-1,6,11,16-tetraazaporphyrinogen, Tz (see below), has been chosen. The reason lies in the flexibility[8] and in the size of cavity of this ligand, which allows the coordination of different metal ions.[9]

Tz:
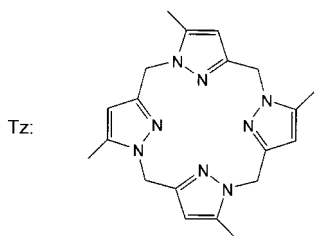
In this paper we report on the compounds obtained by the reaction of the metal–macrocycle [M(Tz)]²⁺, (M = Cu, Ni) and TCNQ in different oxidation states. Radical-ion salts of formula [M(Tz)(MeOH)₂](TCNQ)₂ are prepared by reaction of the perchlorate salt, that is [M(Tz)](ClO₄)₂, and of Li[TCNQ], while radical-ion salts of formula [M(Tz)]₂(TCNQ)₇ (M = Cu, Ni) are obtained by starting from the mixed-valence (Et₃NH)[TCNQ]₂ as acceptor.

Results and Discussion

The reaction of [M(Tz)](ClO₄)₂ with LiTCNQ or (Et₃NH)(TCNQ)₂ takes place with displacement of the counter anion by two organic radicals. No appreciable charge transfer is observed between the organic acceptor molecule and the metal ion, which retains the +2 oxidation state. In the case of the reaction with LiTCNQ, two methanol molecules complete the metal coordinative environment, leaving the radical anions out of the coordination sphere. When the reaction is carried out in the presence of (Et₃NH)[TCNQ]₂, a reagent where the TCNQ units are in a formal average charge of 0.5e, the stoichiometry of the product, that is [M(Tz)]₂(TCNQ)₇ (M = Cu, Ni), indicates that, for electroneutrality requirements, there must be four anionic TCNQ and the other three organic acceptors should be neutral.

Crystal structure of [Cu(Tz)(MeOH)₂](TCNQ)₂: The compound crystallizes in the monoclinic system, space group P2₁/n. An ORTEP view of the molecular unit is shown in Figure 1.

The crystal structure can be described as being formed by the alternation of cations [Cu(Tz)(MeOH)₂]²⁺ and dianions [TCNQ]₂²⁻. The copper(II) ion is six-coordinate in a tetragonally elongated octahedral environment with the four nitrogen atoms of the Tz macrocyclic ligand in the equatorial plane with Cu−N bond lengths in the range 1.91–1.96 Å. The two methanol molecules complete the coordination environment in apical positions with bond lengths Cu−O(1), 2.46 and Cu−O(2), 2.51 Å. Due to the large size of the macrocyclic cavity, which makes it able to host a second row transition metal ion,[9] the macrocycle is shrunk to fit around the smaller copper ion. The [CuN₄] moiety is not planar but has the four nitrogen atoms deviated by an average of 0.02 Å above the best least-square plane, which contains the copper atom,
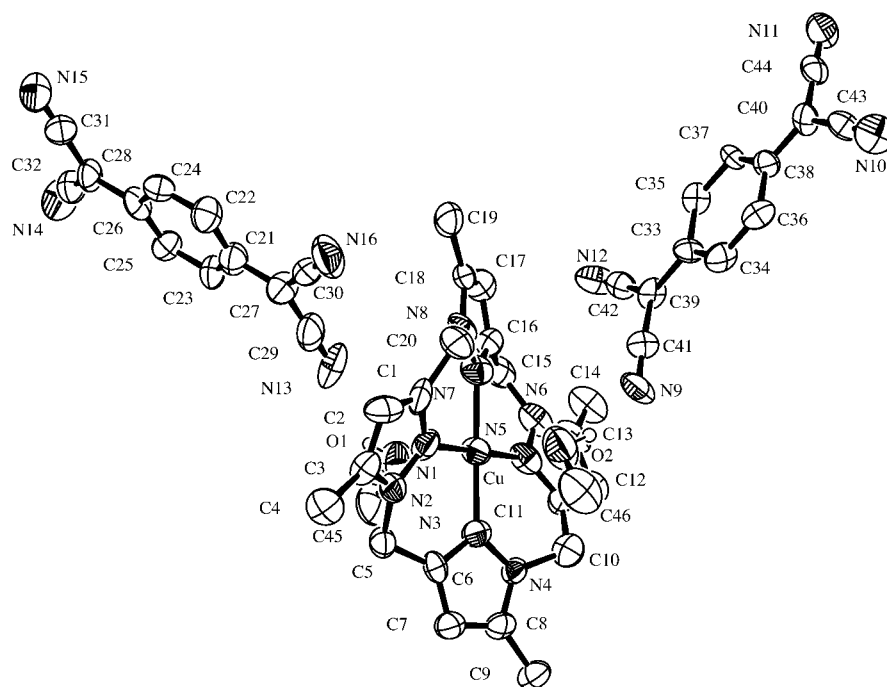

Figure 1. ORTEP view (50% probability ellipsoids) of [Cu(Tz)(MeOH)₂](TCNQ)₂.

pushing away one coordinated methanol group (Figure 2). The four pyrazole groups are planar and twisted with respect to the [CuN₄] equatorial plane by an average of 21.5°.
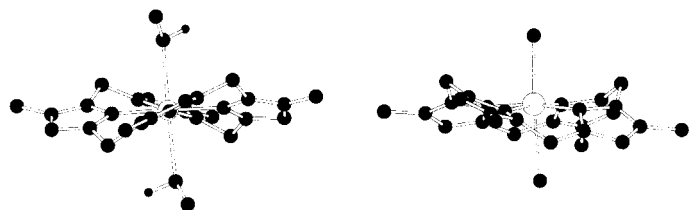

Figure 2. View of the [Cu(Tz)] unit showing the fitting of the macrocycle to the copper atom in [Cu(Tz)(MeOH)₂](TCNQ)₂, left, and [Cu(Tz)]₂(TCNQ)₇, right.

Figure 3. View of the crystal packing in [Cu(Tz)(MeOH)₂](TCNQ)₂ (○ TCNQ A, ● TCNQ B atoms).

There are two crystallographically non equivalent TCNQ molecules in the unit cell, identified as TCNQ A and TCNQ B. The metallomacrocyclic cation has a 2+ charge and therefore all the TCNQ in the crystal must be mono-anionic. A linear relation between the carbon–carbon bond lengths of the TCNQ and the degree of charge held on this molecule has previously been observed,[10] but unfortunately the poor quality of the crystal studied precludes the determination of this degree of charge from the experimental data. Each TCNQ is related with an adjacent radical anion by an inversion center. These two anions overlap their π clouds forming dimeric dianions. The overlap mode is of the ring-over-ring mode[3a] for the TCNQ A dimer, while it is of the ring-over-external-bond mode for the TCNQ B dimer. The observed intra-dimer distances, that is 3.23(4) and 3.13(4) Å, respectively, are typical of these dimeric species.[4, 5]

The crystal packing (Figure 3) shows that the cationic metallomacrocycle and the dianions [TCNQ]₂²⁻ are joined together by hydrogen bonds between one of the nitrile groups of every TCNQ and the hydroxo group of the methanol ligands. TCNQ A, forms a hydrogen bond with O1, O1–H01 0.94(2), H01···N13 2.00(3) Å, angle O1–H01–N13 142(1)°. In a similar way, TCNQ B is hydrogen bonded to the other methanol group, O2–H02 1.02(1), H02···N9 1.90(3) Å, angle O2–H02–N9 142(1)°. Due to the centrosymmetric nature of the [TCNQ]₂²⁻ dimer each unit forms a hydrogen bond with a

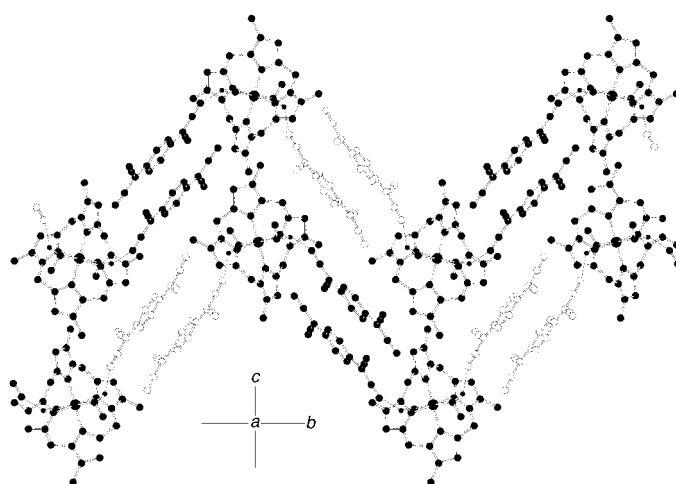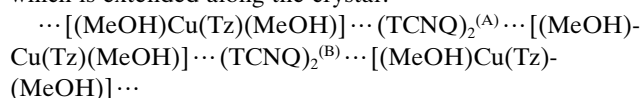different metallomacrocyclic cation, originating a zigzag chain which is extended along the crystal:

···[(MeOH)Cu(Tz)(MeOH)]···(TCNQ)₂⁽ᴬ⁾···[(MeOH)-Cu(Tz)(MeOH)]···(TCNQ)₂⁽ᴮ⁾···[(MeOH)Cu(Tz)-(MeOH)]···

Crystal structure of [Cu(Tz)]₂(TCNQ)₇: An ORTEP view of the formula unit is reported in Figure 4. Table 1 shows the most significant bond lengths and angles. The structure consists of infinite one-dimensional stacks of TCNQ units, with the metallomacrocycles located in between the stacks. The copper atom is six-coordinated in a very distorted environment. The Tz ligand is located in the equatorial plane with four Cu–N distances of 1.95–1.97 Å in the usual range found for sp² nitrogens.[11] The coordination around the copper ion is completed by two nitrile groups of two TCNQ units bonded in apical positions. One Cu–N distance is 2.442(6) Å while the other is much longer, 2.707(4) Å. This distortion of the coordination environment can be attributed to steric hindrance of the macrocyclic ligand. In contrast to the observed shrink in [Cu(Tz)(MeOH)₂](TCNQ)₂ the macrocycle is now folded in one direction (Figure 2) with the copper atom located 0.138(3) Å above the plane defined by the four
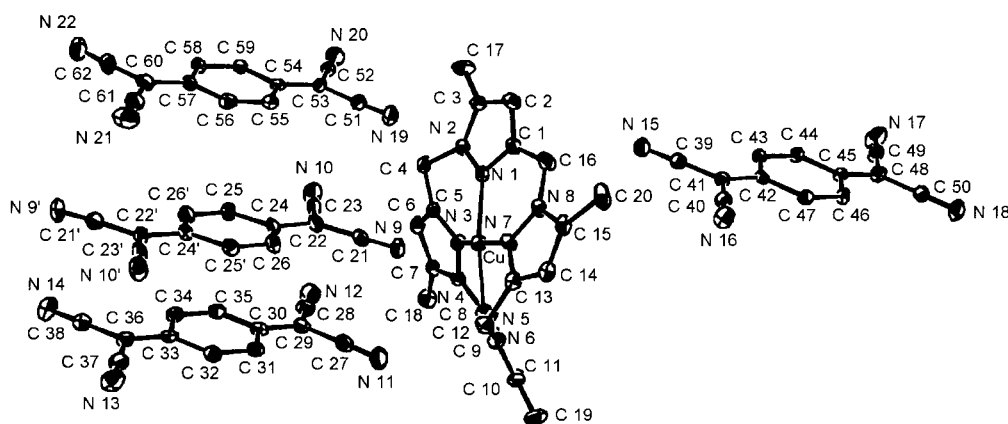

Figure 4. ORTEP view (50% probability ellipsoids) of [Cu(Tz)]₂(TCNQ)₇.

Table 1. Selected bond lengths [Å] and angles [°] for [Cu(Tz)₂](TCNQ)₇.

Bond lengths			Bond angles
Cu−N1 1.976(5)	C30−C31 1.423(9)	C45−C46 1.434(8)	N3-Cu-N7 172.2(2)
Cu−N3 1.963(5)	C30−C35 1.430(9)	C46−C47 1.346(8)	N3-Cu-N1 89.2(2)
Cu−N5 1.988(5)	C31−C32 1.348(9)	C48−C50 1.429(8)	N7-Cu-N1 88.8(2)
Cu−N7 1.970(5)	C32−C33 1.422(9)	C48−C49 1.430(9)	N3-Cu-N5 88.98(2)
Cu−N9 2.442(6)	C33−C36 1.380(9)	N19−C51 1.149(8)	N7-Cu-N5 91.9(2)
Cu−N18 2.707(4)	C33−C34 1.437(9)	N20−C52 1.143(8)	N1-Cu-N5 171.8(2)
N9−C21 1.143(7)	C34−C35 1.349(9)	N21−C61 1.163(10)	N3-Cu-N9 90.83(2)
N10−C23 1.133(8)	C36−C37 1.438(10)	N22−C62 1.157(10)	N7-Cu-N9 96.8(2)
C21−C22 1.429(9)	C36−C38 1.441(9)	C51−C53 1.435(9)	N1-Cu-N9 96.43(2)
C22−C24 1.412(9)	N15−C39 1.140(7)	C52−C53 1.438(10)	N5-Cu-N9 91.6(2)
C22−C23 1.429(10)	N16−C40 1.134(8)	C53−C54 1.388(8)	N2-N1-Cu 124.8(4)
C24−C25 1.430(9)	N17−C49 1.144(8)	C54−C59 1.437(8)	N4-N3-Cu 126.4(4)
C24−C26 1.411(9)	N18−C50 1.143(7)	C54−C55 1.438(8)	N6-N5-Cu 122.7(4)
C25−C26 1.363(9)	C39−C41 1.428(8)	C55−C56 1.351(9)	N8-N7-Cu 126.8(4)
N11−C27 1.139(7)	C40−C41 1.434(9)	C56−C57 1.432(9)	C21-N9-Cu 140.2(5)
N12−C28 1.146(8)	C41−C42 1.400(8)	C57−C60 1.393(9)	
N13−C37 1.139(9)	C42−C47 1.434(7)	C57−C58 1.400(9)	
N14−C38 1.137(8)	C42−C43 1.431(7)	C58−C59 1.347(9)	
C27−C29 1.432(9)	C43−C44 1.354(8)	C60−C61 1.430(12)	
C28−C29 1.441(10)	C44−C45 1.424(8)	C60−C62 1.433(11)	
C29−C30 1.390(9)	C45−C48 1.388(8)		

macrocyclic nitrogens. This folding allows one TCNQ to get closer to the copper atom, while the other TCNQ is taken away from the copper due to the hindrance of the macrocycle in that direction.

The seven TCNQ molecules found in the unit cell belong to four crystallographically different types. There is one unique TCNQ, labeled TCNQ A, located on an inversion center, while there are two molecules of the other three types, TCNQ B, C, and D. All the TCNQ molecules are stacked by overlap of their π-electron clouds. The TCNQ molecules labeled A and D are coordinated to the copper(ii) ions through the N atom of the nitrile group and that of TCNQ A shows the shortest bond lengths to the copper atom. Due to its centrosymmetry it is also acting as a bridge between two [CuTz] moieties. The long Cu−N bond corresponds to TCNQ D, which acts as a monodentate ligand. This unit is related by an inversion center to an adjacent TCNQ D molecule; both TCNQ groups overlap in the ring over external bond modes with an interplanar distance of 3.37(1) Å. This pair of overlapping TCNQ is also bridging two different [CuTz] moieties (Figure 5).

The two TCNQ B molecules overlap with TCNQ A, above and below its molecular plane, in the ring-over-ring mode with a shortest intermolecular distance of 3.42(1) Å. TCNQ C

molecules are located between TCNQ B and D and overlap with both units in the ring-over-external bond mode, with distances of 3.40(1) Å between TCNQ B and C and 3.37(1) Å between TCNQ C and D. Both TCNQ B and C are uncoordinated.
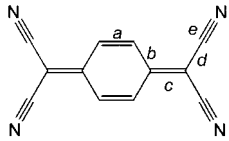
The repeating pattern along the TCNQ stack is therefore -A-B-C-D-D-C-B-A- (Figure 5). All the TCNQ are almost parallel with angles between planes of 3.4(2)° between TCNQ A and B, 3.4(2)° between TCNQ B and C, and 1.2(2)° between TCNQ C and D. The interplanar distances are slightly longer than those usually found in dimeric species.[4, 5] This fact is interpreted in terms of delocalization of the electron density along the chain,[7] requiring the presence of TCNQ molecules bearing fractional charges. As mentioned previously, the charge of the TCNQ molecules can be related to the variation of the C−C bond lengths on reduction. The extra electron occupies an anti-bonding orbital and this is reflected in a lengthening of the quinoid (c) bond. By using a linear relation between the electronic charge located in the TCNQ and the variation of the C−C bond lengths[10b] we have found that TCNQ A is monoanionic, thus bearing one of the four negative charges
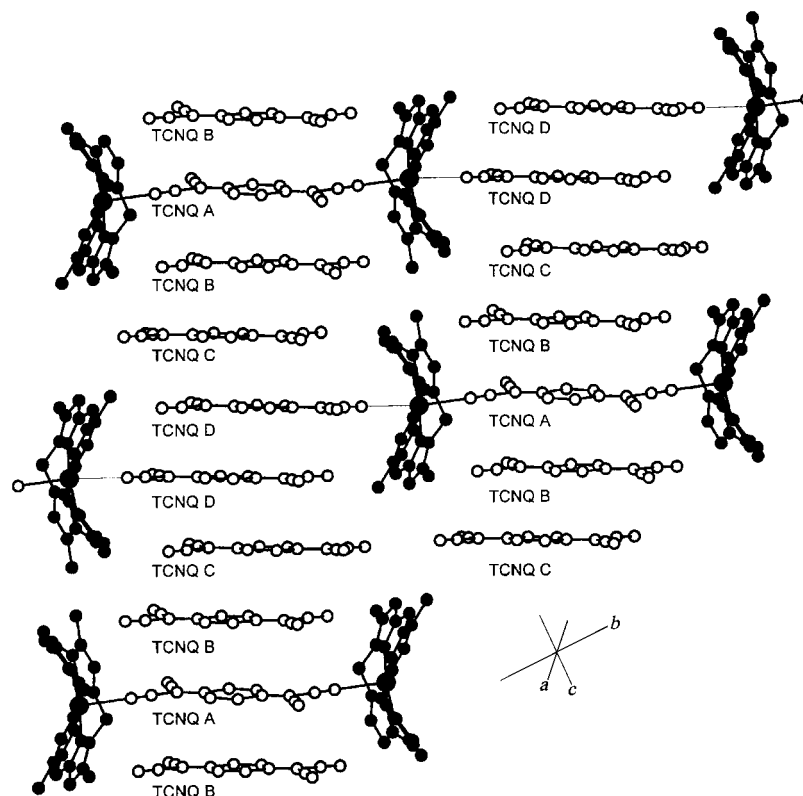
Figure 5. View of the TCNQ stack in [Cu(Tz)]₂(TCNQ)₇.

distributed between the seven TCNQ in the cell unit (Table 2). The other six TCNQ have similar parameters and, within experimental error, they correspond to a formal

Table 2. Comparative analysis of the TCNQ bond lengths [Å] in [Cu(Tz)$_2$](TCNQ)$_7$.

Compound	a	b	c	d	b−c	c−d	c/(b + d)
TCNQ$^{0\,[a]}$	1.345	1.448	1.374	1.441	0.074	− 0.067	0.476
TCNQ$^{-\,[a]}$	1.373	1.423	1.420	1.416	0.003	0.004	0.500
TCNQ$^{0.5-\,[a]}$	1.354	1.434	1.396	1.428	0.040	− 0.032	0.488
TCNQ A	1.363	1.421	1.412	1.429	0.009	− 0.017	0.495(6)
TCNQ B	1.348	1.428	1.385	1.438	0.043	− 0.053	0.483(6)
TCNQ C	1.349	1.427	1.391	1.434	0.036	− 0.043	0.486(6)
TCNQ D	1.350	1.431	1.394	1.430	0.037	− 0.036	0.487(6)

[a] Ref. [18].

average charge of 0.5e, and indicate that the three electrons are delocalized over the six TCNQ of the chain fragment B-C-D-D-C-B. TCNQ A, bearing one localized electron, separates these areas of delocalization. This picture should correspond to a good semiconductor with some electronic delocalization along the TCNQ stack: the d.c. electrical conductivity value measured on a powdered sample at room temperature was 0.82 S cm^{-1} and the activation energy 0.044 eV, in the temperature range 150–300 K, confirming this assumption.

Spectroscopic properties: The IR spectra are a very useful source of information for TCNQ radical ion salts: they give an indication of the presence of TCNQ in neutral and/or reduced forms as well as the coordinative status of these organic acceptor molecules.[12] The most characteristic bands of neutral TCNQ are the $\tilde{v}(CN) = 2228$, $\tilde{v}_{20}(b_{1u}) = 1530$, $\tilde{v}_4(a_g) = 1424$, and $\tilde{v}_{50}(b_{3u}) = 860$ cm^{-1}, the latter assignable to a C−C stretching and an out-of-plane bending mode. In the case of the monoanion [TCNQ]$^-$ these bands are shifted to lower frequencies, appearing at 1507, 1386 and 824 cm^{-1}, respectively, and a linear relation between the frequency of either $\tilde{v}_{20}$, $\tilde{v}_4$ or $\tilde{v}_{50}$ and the

charge held on the TCNQ has been proposed.[12b, 13] In the radical anion the $\tilde{v}(CN)$ band is also shifted to lower frequencies (2194/2177 cm^{-1}) and split into two or three components due to a lowering of symmetry in the nitrile groups. The IR spectra of [M(Tz)(MeOH)$_2$](TCNQ)$_2$ show typical bands of the TCNQ in its mono-anionic form with the above-mentioned bands appearing at 2184, 2155, 1506, and 826 cm^{-1} for the nickel derivative and at 2191, 2164, 1507, and 823 cm^{-1} for the copper one, in complete accordance with the crystallographic results.

The IR spectra of both [M(Tz)]$_2$(TCNQ)$_7$ derivatives are identical but they show completely different features from those of the [M(Tz)(MeOH)$_2$](TCNQ)$_2$ compounds. The most pronounced characteristic is that they show broad vibrational bands superimposed on an electronic absorption background, a typical feature of derivatives with a degree of electronic delocalization along the TCNQ stacks.[14] This electronic absorption is observed in the visible-NIR spectrum centered at 5200 cm^{-1} and can be assigned to the low energy charge-transfer transition, CT$_2$, between radical anion and neutral TCNQ.[15]

The most significant bands of [Cu(Tz)]$_2$(TCNQ)$_7$ (Figure 6) are observed at 2154, 2168, and 2178 with a shoulder at
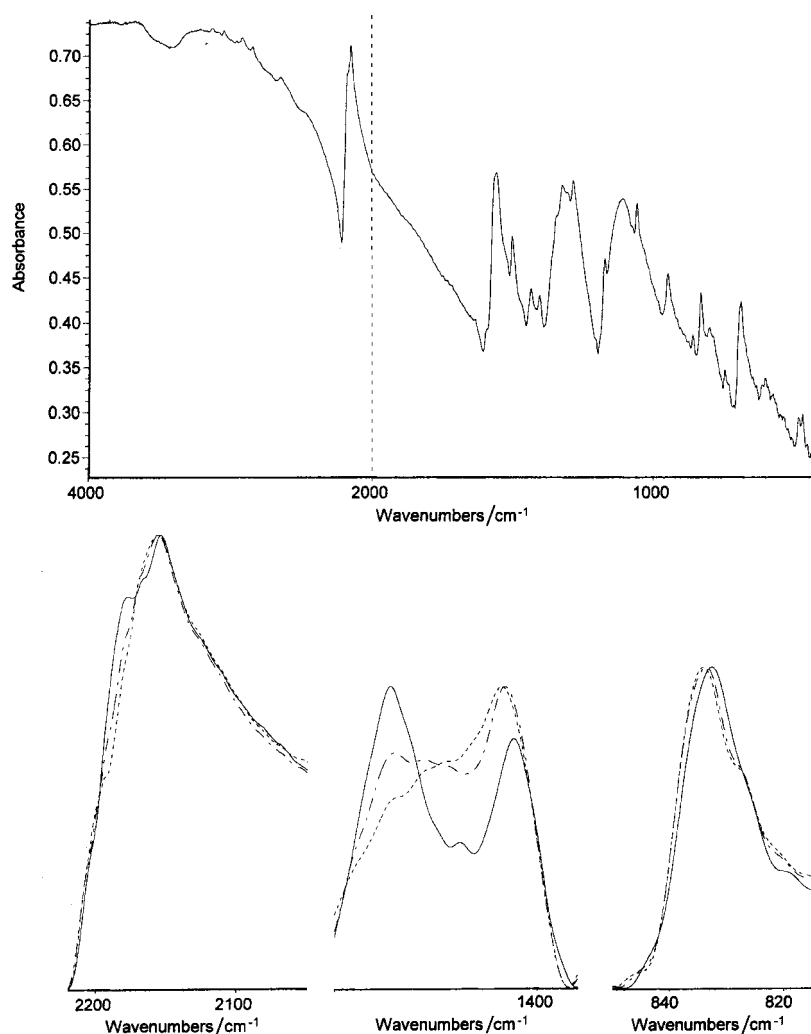

Figure 6. IR spectrum of [Cu(Tz)]$_2$(TCNQ)$_7$. The expanded regions show the spectra at 300 K (——), 120 K (•—•—) and 8 K (----).

2210 cm^{-1} for the $\tilde{v}$(CN) bands, 1505 cm^{-1} for the $\tilde{v}_{20}$ mode with a weak shoulder at 1524 cm^{-1}, and 834 cm^{-1} for the $\tilde{v}_{50}$ mode. This spectrum is very similar to those of other derivatives having TCNQ units that bear formal fractional negative charges,[7c] and the frequency of the $\tilde{v}_{20}$ (at 1524 cm^{-1}) and $\tilde{v}_{50}$ vibrational modes agree with the assignment of 0.5 electrons per TCNQ made, as confirmed by the crystal structure. The $\tilde{v}_{20}$ band at 1505 cm^{-1} is also coherent with the presence of uninegative TCNQ, as the crystal structure confirms. The different coordination modes observed in the crystal would be responsible for the appearance of several $\tilde{v}$(CN) bands due to nitrile groups in different environments.

The variation of this IR spectrum with temperature has also been studied in an attempt to identify possible phase transitions that would change the TCNQ stack. Figure 6b shows the regions where changes with the temperature are observed. For the sake of clarity only the spectra at higher and lower temperatures and one intermediate are shown.

In the $\tilde{v}$(CN) region the band at 2168 cm^{-1} gradually disappears while a new band at 2193 cm^{-1} is observed. In the $\tilde{v}_4$ region new bands at 1428 and 1423 cm^{-1} grow between those previously observed at 1437 and 1408 cm^{-1}. Finally, the $\tilde{v}_{50}$ band shows a shoulder at 827 cm^{-1} along with the primitive band at 834 cm^{-1}. No appreciable changes are observed in the $\tilde{v}_{20}$ region. From the gradual shift in frequencies and intensities of these bands we can conclude that no sharp phase transition is observed; rather, a smooth localization of the electronic charge on some TCNQ units, accompanied or not by small changes in coordination to the metal, seems more probable.

The EPR spectra of the four reported compounds have been recorded on powdered samples at room temperature. The spectrum of [Ni(Tz)(MeOH)$_2$](TCNQ)$_2$ shows only one signal centered at $g = 2.0027$ ($\Delta H = 7.7$ G); this signal can be attributed to the unpaired electrons located on TCNQ molecules. No signal from Ni^{II} is observed, as expected, due to the rapid relaxation of the S $= 1$ state for six-coordinate nickel(II).[16]

The EPR spectrum of [Cu(Tz)(MeOH)$_2$](TCNQ)$_2$ (Figure 7a) shows a broad line due to Cu^{II} and a sharp one ($g = 2.0032$, $\Delta H = 1$ G) attributed to TCNQ. The copper signal corresponds to an axial symmetry with hyperfine structure with the following parameters: $g_{\parallel} = 2.18$, $g_{\perp} = 2.03$, $A_{\parallel} = 210$ G, $A_{\perp} = 20$ G. The pattern and g values are characteristic of tetragonally elongated octahedral copper(II).[17] The spectrum of [Cu(Tz)]$_2$(TCNQ)$_7$ shows similar features (Figure 7b) and has axial symmetry, but the signals are not resolved for hyperfine coupling. This fact suggests a very different environment for the copper atom, also indicated by the different g values found for this compound: $g_{\parallel} = 2.10$, $g_{\perp} = 2.03$. The TCNQ signal appears at $g = 2.0025$ and shows a double peak (Figure 7b inset) that could be attributed to a uniaxial orientation of the TCNQ in the complex. The analogous nickel derivative shows only the TCNQ radical signal at $g = 2.0028$ ($\Delta H = 2$ G), also split in an axial fashion.

Magnetic properties: The bulk d.c. magnetic susceptibility has been measured on a polycrystalline sample over the range 2 – 300 K for the studied compounds. The χT versus temperature
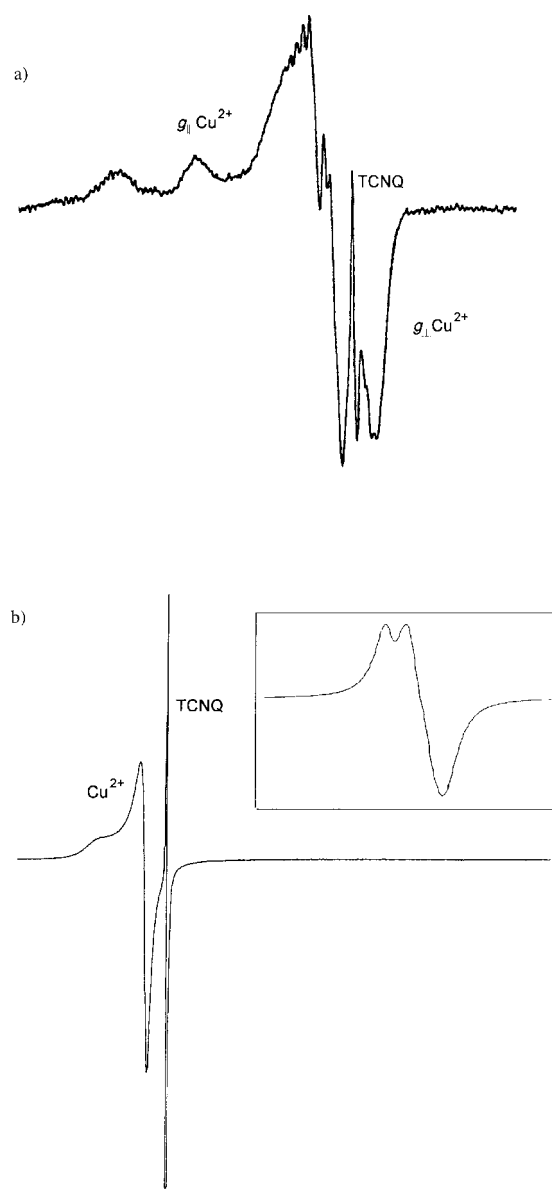

Figure 7. EPR spectra of solid samples of a) [Cu(Tz)(MeOH)$_2$](TCNQ)$_2$, and b) [Cu(Tz)]$_2$(TCNQ)$_7$. Inset: the TCNQ signal.

plot of compound [Cu(Tz)(MeOH)$_2$](TCNQ)$_2$ follows the Curie–Weiss law (Figure 8), with a Curie constant, C, of 0.393 cm^3 K mol^{-1} and a θ value of -1.24 K, corresponding to an effective magnetic moment of 1.77 μ_B, thus indicating that the magnetic behavior originates only from isolated metal centers, because of the strong antiferromagnetic coupling inside the TCNQ dimers. The corresponding nickel analog also exhibits a similar magnetic behavior, arising only from isolated nickel(II), S $= 1$ spins. In fact, the data above 50 K fit the Curie law with a Curie constant of 0.961 cm^3 K mol^{-1}, corresponding to an effective magnetic moment of 2.77 μ_B. Below 50 K the data deviate from the Curie law and this deviation can be ascribed to the presence of zero-field splitting, which is one of the most important sources of magnetic anisotropy in nickel(II) octahedral derivatives.[19] Equation (1) takes into account this single-ion anisotropy for the average magnetic susceptibility, where $x = D/kT$, the
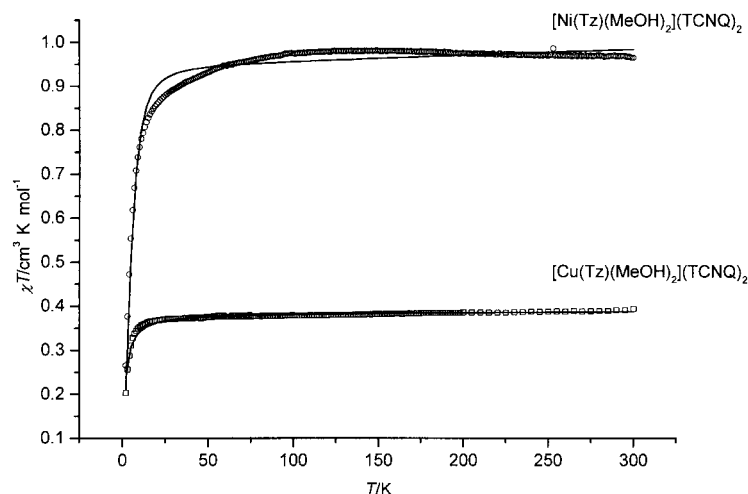
Figure 8. Temperature dependence of χT for $[M(Tz)(MeOH)_2](TCNQ)_2$, M = Cu, Ni. The solid lines represent the fitting of the data as discussed in the text.

parameter D measures the zero-field splitting for the ground state:

$$\langle\chi\rangle = \frac{C}{T}\frac{[2 - 2\exp(-x)]/x + \exp(-x)}{[1 + 2\exp(-x)]} \tag{1}$$

The best fit to the experimental data (Figure 8) gives the parameters $C = 0.943$ cm^3 K mol^{-1} and $D = 12.5$ cm^{-1}. The Curie constant does not differ significantly from the high temperature value, while the D parameter indicates that anisotropy is found in the nickel environment.

The magnetic susceptibility of $[Cu(Tz)]_2(TCNQ)_7$ has been measured in the temperature range 5–300 K at an external field of 5000 Oe. The effective magnetic moment, calculated from the equation $\mu_{eff} = 2.83(\chi T)^{1/2}$, steadily increases from $1.82\mu_B$ at 3 K to $3.12\mu_B$ at 300 K (Figure 9). These values suggest that at lower temperatures only the metal ion contributes to the magnetic susceptibility with the spins on the TCNQ strongly antiferromagnetically coupled and that at high temperatures four S = ½ spins, together with that of the Cu^{II}, are present in the formula unit. The field dependence of the magnetization at 5 K is reported in Figure 10. The
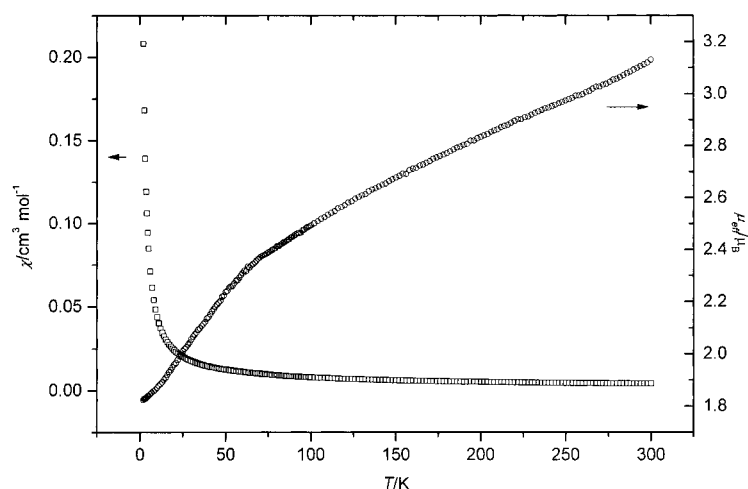
experimental data fit well to the Brillouin function for a S = ½ paramagnet with a g value of 2.094(2), in good agreement with the EPR data. Assuming that the copper ions would follow the Curie law, this g value corresponds to a Curie constant of 0.4114 cm^3 K mol^{-1}.

On the basis of the crystal structure and the above observations, the magnetic properties of $[Cu(Tz)]_2(TCNQ)_7$ can be interpreted as the sum of three contributions:

$$\chi_M = \chi_{Cu} + \chi_{org} + N\alpha \tag{2}$$

where χ_{Cu} is the Curie contribution arising from the uncorrelated Cu^{II} (S = ½) spins, χ_{org} is the contribution of the spins located on the TCNQ stacks, and $N\alpha$ is the temperature-independent paramagnetism (TIP). Now, if the metal-ion contribution and the TIP are subtracted from the total magnetic susceptibility, a typical χ_{org} versus T plot of one-dimensional antiferromagnetic chains of S = ½ spins is observed (Figure 11).[20]

The copper contribution has been estimated from the C/T equation, and by using the value for the Curie constant as obtained from the fit of the Brillouin function. The TIP contribution can be estimated by plotting χ versus $1/T$, and extrapolating the susceptibility value for $T \rightarrow \infty$; this gives a value of 2.3×10^{-3} cm^3 mol^{-1}. This relatively high TIP contribution may have different contributions, besides the TIP contribution of the copper(II) ions (on the order of 6×10^{-5} cm^3 mol^{-1}), a Pauli paramagnetic contribution coming from the delocalized electrons on the anion-radicals, as has been observed in other conducting radical-ion salts.[21]

The temperature dependent susceptibility of the organic part obtained in this way is reported in Figure 11. It shows a broad maximum centered at $T_{max} \approx 54$ K, a typical signature of a one-dimensional S = ½ spin system. The experimental data above T = 15 K were then fitted to a Heisenberg linear chain model with the Equation (3) derived from Hatfield et al.:[20]

$$\chi_{org} = \frac{Ng^2\beta^2}{kT}\frac{A + Bx + Cx^2}{1 + Dx + Ex^2 + Fx^2} \tag{3}$$

where $x = |J|/kT$ and A, B, C, D, E, and F are functions of α, a parameter that takes into account the distortion in the chain and can vary from $\alpha = 0$ (corresponding to isolated TCNQ$^{\cdot-}$ dimers) to $\alpha = 1$ (corresponding to a uniform chain of S = ½ spins). The best fit of the experimental results was obtained by using $g = 2.0025$, taken from the EPR spectrum, and affords $J = -37.3(1)$ cm^{-1} and $\alpha = 0.91$, suggest-

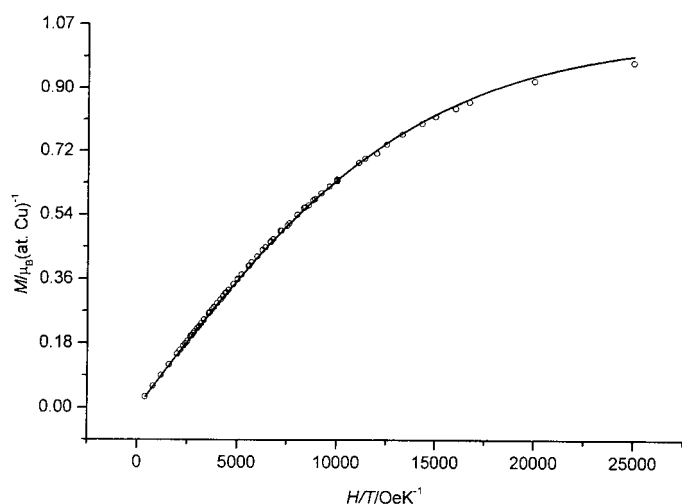Figure 9. Temperature dependence of the static molar susceptibility and the effective magnetic moment of $[Cu(Tz)]_2(TCNQ)_7$ in the temperature range 5–300 K.

Figure 10. Field dependence of the magnetization at $T = 5$ K for [Cu(Tz)]$_2$(TCNQ)$_7$. The solid line represents the fit of the data to the Brillouin function of a S = ½ paramagnet with $g = 2.094$.
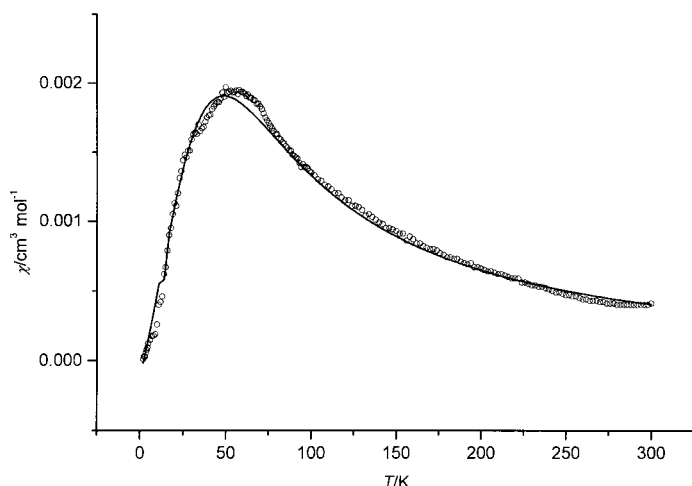

Figure 11. Plot of the magnetic susceptibility of the organic part of [Cu(Tz)]$_2$(TCNQ)$_7$ as a function of the temperature. The solid line is the fit to the experimental data (see text).

nickel ions contribute to the total magnetic susceptibility at low temperatures and the magnetic anisotropy is present, the data below 30 K were fitted to Equation (1), obtaining $C = 0.921$ cm^{3}K mol^{-1} and $D = 7.8$ cm^{-1}. The TIP contribution for this compound was estimated in the same way to that mentioned above for the copper derivative, and a value of 1.74×10^{-3} cm^3 mol^{-1} was found. The magnetic susceptibility was then assumed to be the sum of the contributions of the isolated S = 1 nickel(II) ions, the contribution of the spins located on the TCNQ, and that of the TIP.

$$\chi_{\text{total}} = \chi_{\text{Ni}} + \chi_{\text{org}} + N\alpha \tag{4}$$

where χ_{Ni} and χ_{org} are expressed by Equations (1) and (3), respectively. After subtraction of the nickel and TIP contributions from the total magnetic susceptibility, the magnetic susceptibility contribution of the organic part was then obtained. Unfortunately, the crystal structure of this compound is unknown, and an attempt was made by assuming for the nickel analogue a similar one-dimensional magnetic chain structure to that found in the copper analogue. The data were fitted to Equation (3) and the parameter α varied, but the fit was poor.

Conclusion

Two different types of metal – porphyrinogen – TCNQ radical-ion salts have been isolated and characterized. The flexibility of the Tz macrocycle, able to accommodate around the metal atom, allows the formation of completely different architectures. Single-valence derivatives of formula [M(Tz)(MeOH)$_2$](TCNQ)$_2$ were obtained by reaction of [M(Tz)](ClO$_4$)$_2$ and LiTCNQ, while mixed-valence radical-ion salts of formula [M(Tz)]$_2$(TCNQ)$_7$ were obtained by reaction of [M(Tz)](ClO$_4$)$_2$ and (Et$_3$NH)[TCNQ]$_2$. While the former structure consists of the well known alternating dimeric dianions [TCNQ]$_2^{2-}$ and metallomacrocyclic cations, the crystal structure of the [Cu(Tz)]$_2$(TCNQ)$_7$ consists of segregated TCNQ stacks with a certain degree of electronic

ing the presence of a slightly distorted magnetic chain, in agreement with the structural data.

The magnetic susceptibility of [Ni(Tz)$_2$](TCNQ)$_7$ has also been measured in the temperature range 2 – 300 K at an external field of 0.3 T and is reported in Figure 12. The effective magnetic moment, calculated from the equation $\mu_{\text{eff}} = 2.83(\chi T)^{1/2}$, steadily increases from $\approx 1 \mu_B$ at 2 K to 7 μ_B at 300 K. At higher temperatures, four S = ½ spins and one S = 1 spin are present in the formula unit, and at low temperatures only that arising from the nickel(II) ions is observed. Assuming that only the
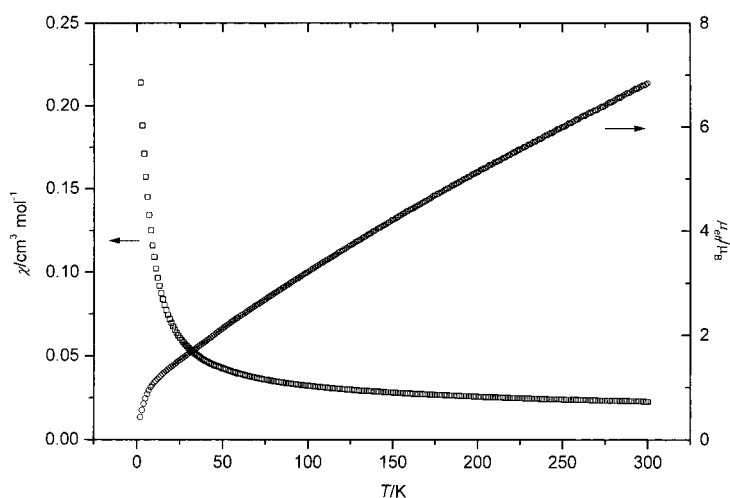

Figure 12. Temperature dependence of the static molar susceptibility and the effective magnetic moment of [Ni(Tz)]$_2$(TCNQ)$_7$ in the temperature range 2 – 300 K.

delocalization along them separated by [Cu(Tz)] units. The formula and structure of this species is unprecedented since the most common architecture found for delocalized TCNQ stacks corresponds to the overlap of trimeric $[TCNQ]_3^{2-}$ anions in derivatives of formula $[ML_n](TCNQ)_3$.[7] The formation of $[Cu(Tz)]_2(TCNQ)_7$, with one extra TCNQ every two metallomacrocyclic units, can be attributed to the large size of the porphyrinogen macrocycle: in fact the adjacent [Cu(Tz)] units are separated by only 3.64 Å (distance between C18 and C19 of adjacent macrocycles). If we keep the same structural arrangement and remove one TCNQ to form a hypothetical $[Cu(Tz)]_2(TCNQ)_6$, the intermolecular TCNQ-TCNQ space along the stack would increase excessively to allow an effective π overlap or, alternatively, if this π overlap is maintained, it would imply extremely short contacts between neighboring metallomacocycles. As a consequence of the new stoichiometry, the electronic delocalization along this stack is greater than that found previously in other metallomacrocycle-TCNQ derivatives. The magnetic behavior could be described as the sum of the Curie contribution of the Cu(II) complex units and the antiferromagnetic exchange interactions between the nearest-neighbor TCNQ spins along the chains. This interaction can be fitted using a 1D Heisenberg alternating chain model: the compound behaves like a distorted 1D magnetic chain of $S = \frac{1}{2}$ spins, in agreement with the structural data. $[Ni(Tz)]_2(TCNQ)_7$ has also been prepared and isolated as microcrystalline powder, but no structural information is available. The compound is a semiconductor, and an attempt to understand the magnetic behavior by using the same model applied to the copper analog is not completely satisfactory.

Experimental Section

All the reactions have been carried out under an inert atmosphere. Tz,[22] LiTCNQ,[23] and (Et$_3$NH)[TCNQ]$_2$[23] were obtained according to published methods and their purities checked by elemental analyses. Perchlorate salts, being potentially explosive, were used in small amounts and handled with care.

[M(Tz)](ClO$_4$)$_2$ (M = Cu, Ni): A MeOH solution (15 mL) of the macrocycle (0.38 g, 1 mmol) was added to a stirred solution of M(ClO$_4$)$_2$·6H$_2$O (0.36 g, 1 mmol) in MeOH (30 mL). After ten minutes of stirring, the solid obtained was filtered off, washed with methanol and dried. Yield: almost quantitative.

[M(Tz)(MeOH)$_2$](TCNQ)$_2$ (M = Cu, Ni): A MeOH solution (40 mL) of LiTCNQ (0.07 g, 0.34 mmol) was added dropwise to a stirred solution of [M(Tz)](ClO$_4$)$_2$ (0.1 g , 0.17 mmol) in acetonitrile (20 mL). The resulting solution was cooled at −20 °C for two days, and dark green crystals that formed were filtered off, washed with methanol and dried under vacuum. Yield: 68 %.

[Cu(Tz)(MeOH)$_2$](TCNQ)$_2$: IR (KBr): $\tilde{v}$ = 3440 m, 2201 s, 2191 vs, 2164 s, 1578 s, 1507 s, 1478 w, 1364 m, 1332 s, 1225 s, 1181 s, 988 w, 823 m, 720 w, 481 cm^{-1} w; elemental analysis calcd (%) for CuC$_{46}$H$_{40}$N$_{16}$O$_2$: C 60.6, H 4.4, N 24.6; found: C 60.3, H 4.4, N 24.6.

[Ni(Tz)(MeOH)$_2$](TCNQ)$_2$: IR (KBr): $\tilde{v}$ = 3436 m, 2184 vs, 2176 s, 2155 s, 1582 s, 1506 s, 1434 w, 1403 w, 1357 m, 1339 m, 1280 m, 1183 m, 1175 s, 1058 w, 1029 w, 826 w, 795 cm^{-1} w; elemental analysis calcd (%) for NiC$_{46}$H$_{40}$N$_{16}$O$_2$: C 60.9, H 4.4, N 24.7; found: C 60.6, H 4.4, N 24.6.

[M(Tz)]$_2$(TCNQ)$_7$ (M = Cu, Ni): An acetonitrile solution (15 mL) of (Et$_3$NH)(TCNQ)$_2$ (0.15 g, 0.3 mmol) was added to a solution of [M(Tz)](ClO$_4$)$_2$ (0.07 g, 0.12 mmol) in acetonitrile (15 mL). The mixture was cooled for three days; dark blue crystals of the title compound

separated, and were filtered off, washed with methanol and dried in vacuo. Yield: 74 %.

[Cu(Tz)]$_2$(TCNQ)$_7$: IR (KBr): $\tilde{v}$ = 2178 vs, 2168 vs, 2154 vs, 1560 s, 1526 m, 1505 s, 1437 m, 1408 m, 1322 s, 1287 s, 1113 s, 1058 m, 952 w, 834 m, 805 w, 696 m, 601 w, 482 cm^{-1} w; elemental analysis calcd (%) for CuC$_{62}$H$_{38}$N$_{22}$: C 64.5, H 3.3 N, 26.7; found: C 64.6, H 3.4, N 26.9.

[Ni(Tz)]$_2$(TCNQ)$_7$: IR (KBr): $\tilde{v}$ = 2177 vs, 2160 vs, 1562 s, 1505 s, 1435 w, 1406 w, 1324 s, 1111 s, 1054 m, 952 w, 832 w, 801 w, 694 m, 600 w, 483 cm^{-1} w; elemental analysis calcd (%) for NiC$_{62}$H$_{38}$N$_{22}$: C 64.8, H 3.3, N 26.8; found: C 65.1, H, 3.4, N, 26.7.

Single-crystal growth: Good quality single crystals of the copper compounds were obtained by slow diffusion of a LiTCNQ or (Et$_3$NH)(TCNQ)$_2$ methanolic solution into an acetonitrile solution of [Cu(Tz)](ClO$_4$)$_2$.

Physical measurements: Elemental analyses were carried out by the Servicio de Microanálisis of the Universidad Complutense de Madrid. IR spectra were recorded as KBr pellets on a Nicolet Magna-550 FT-IR spectrophotometer. Electronic spectra were recorded in the solid state by rubbing the sample on optical glass using a Cary-5 spectrophotometer. Magnetic susceptibility experiments were made on polycrystalline samples using a Quantum Design SQUID magnetometer, Model MPMS-5 S in the temperature range of 2 and 250 K and at constant fields of 0.3 and 0.5 T. Isothermal magnetization as a function of the field up to 5 T was also performed. The experimental data have been corrected for the magnetization of the sample holder and for atomic diamagnetism as calculated from the known Pascal's constants. X-band powder EPR spectra have been obtained on a Bruker ESP 300 apparatus equipped with a Bruker ER 035 M gausometer and an Oxford JTC4 cryostat. Single-crystal electrical conductivity measurements at variable temperature were performed by the four-points method, using an APD cryogenics INCHC 2 helium cryostat.

X-ray Structure determinations: A summary of the fundamental crystal data is reported in Table 3. A green ([Cu(Tz)(MeOH)$_2$](TCNQ)$_2$) or deep-blue ([Cu(Tz)]$_2$(TCNQ)$_7$) crystal of prismatic shape was resin epoxy-coated and mounted on a CAD-4 kappa diffractometer. The cell dimensions were refined by least squares fitting the 2θ values of 25 reflections. The intensities were corrected for Lorentz and polarization effects. Scattering factors for neutral atoms and anomalous dispersion corrections for Cu were taken from ref. [24]. The structures were solved by Patterson and Fourier methods and refined by applying full-matrix least squares on F^2 with anisotropic thermal parameters for the non-hydrogen atoms. The hydrogen atoms were included with fixed isotropic contributions at their calculated positions determined by molecular geometry. The calculations were carried out with the SHELX 97 software package.[25]

CCDC-167164 ([Cu(Tz)]$_2$(TCNQ)$_7$) and CCDC-167165 ([Cu(Tz)-(MeOH)$_2$](TCNQ)$_2$) contain the supplementary crystallographic data for this paper. These data can be obtained free of charge via www.ccdc.cam.

Table 3. Crystal data for [Cu(Tz)(MeOH)$_2$](TCNQ)$_2$ and [Cu(Tz)]$_2$(TCNQ)$_7$.

Compound	[Cu(Tz)(MeOH)$_2$](TCNQ)$_2$	[Cu(Tz)]$_2$(TCNQ)$_7$
empirical formula	C$_{46}$H$_{40}$CuN$_{16}$O$_2$	C$_{62}$H$_{38}$CuN$_{22}$
M_w	912.47	1154.7
crystal system	monoclinic	triclinic
space group	$P2_1/n$	$P\bar{1}$
a [Å]	8.310(2)	11.244(1)
b [Å]	25.180(4)	16.700(1)
c [Å]	20.727(4)	17.321(1)
α [°]		113.47(1)
β [°]	93.58(2)	108.52(1)
γ [°]		96.12(1)
Z	4	2
V [Å^3]	4329(2)	2725(2)
ρ_{calcd} [Mg m^{-3}]	1.40	1.41
T [K]	293	293
λ (Mo$_{K\alpha}$) [Å]	0.71073	0.71073
μ [cm^{-1}]	5.65	4.66
R_1[a]	0.093	0.053
wR_2[b]	0.188	0.150

[a] $R_1 = \Sigma(|F_o| - |F_c|)^2/\Sigma F_o^2$. [b] $wR_2 = \{\Sigma[w(F_o^2 - F_c^2)^2]/\Sigma[w(F_o^2)^2]\}^{1/2}$.

ac.uk/conts/retrieving.html (or from the Cambridge Crystallographic Data Centre, 12 Union Road, Cambridge CB2 1EZ, UK; fax: (+44)1223-336033; or deposit@ccdc.cam.ac.uk).

Acknowledgements

[1] *Handbook of Organic Conductive Molecules and Polymers* (Ed.: H. S. Nalwa), Wiley, Chichester, **1997**.

[2] See for instance M. Kurmoo, A. W. Graham, P. Day, S. J. Coles, M. B. Hursthouse, J. L. Caulfield, J. Singleton, F. L. Pratt, W. Hayes, L. Ducasse, P. Guionneau, *J. Am. Chem. Soc.* **1995**, *117*, 12209, and references therein.

[3] a) H. Endres in *Extended Linear Chain Compounds*, *Vol. 3* (Ed.: J. S. Miller), Plenum, New York, **1982**, p. 263; b) W. Kaim, M. Moscherosch, *Coord. Chem. Rev.* **1994**, *129*, 157; c) L. Ballester, M. C. Barral, A. Gutiérrez, R. Jiménez-Aparicio, J. M. Martínez-Muyo, M. F. Perpiñán, M. A. Monge, C. Ruiz-Valero, *J. Chem. Soc. Chem. Commun.* **1991**, 1396.

[4] a) J. P. Cornelissen, J. H. van Diemen, L. R. Groeneveld, J. G. Haasnot, A. L. Spek, J. Reedijk, *Inorg. Chem.* **1992**, *31*, 198; b) L. Ballester, M. C. Barral, A. Gutiérrez, A. Monge, M. F. Perpiñán, C. Ruiz-Valero, A. Sánchez-Peláez, *Inorg. Chem.* **1994**, *33*, 2142; c) M. T. Azcondo, L. Ballester, A. Gutiérrez, M. F. Perpiñán, U. Amador, C. Ruiz-Valero, C. Bellitto, *J. Chem. Soc. Dalton Trans.* **1996**, 3015; d) L. Ballester, A. Gutiérrez, M. F. Perpiñán, U. Amador, M. T. Azcondo, A. E. Sánchez-Peláez, C. Bellitto, *Inorg. Chem.* **1997**, *36*, 6390.

[5] a) M. C. Muñoz, J. Cano, R. Ruiz, F. Lloret, J. Faus, *Acta Crystallogr. Sect. C* **1995**, 873; b) L. Ballester, A. Gutiérrez, M. F. Perpiñán, M. T. Azcondo, A. E. Sánchez-Peláez, U. Amador, *Anal. Quim. Int. Ed.* **1996**, *92*, 275.

[6] L. Ballester, A. M. Gil, A. Gutiérrez, M. F. Perpiñán, M. T. Azcondo, A. E. Sánchez-Peláez, U. Amador, J. Campo, F. Palacio, *Inorg. Chem.* **1997**, *36*, 5291.

[7] a) L. Ballester, A. Gutiérrez, M. F. Perpiñán, S. Rico, M. T. Azcondo, C. Bellitto, *Inorg. Chem.* **1999**, *38*, 4430; b) M. T. Azcondo, L. Ballester, S. Golhen, A. Gutiérrez, L. Ouahab, S. Yartsev, P. Delhaes, *J. Mater. Chem.* **1999**, *9*, 1237; c) L. Ballester, A. M. Gil, A. Gutiérrez,

[8] C. Floriani, *J. Chem. Soc. Chem. Commun.* **1996**, 1257.

[9] a) C. Marzin, G. Tarragó, M. Gal, I. Zidane, T. Hours, D. Lerner, C. Andrieux, H. Gampp, J. M. Savéant, *Inorg. Chem.* **1986**, *25*, 1775; b) C. Marzin, G. Tarragó, I. Zidane, E. Bienvenue, P. Seta, C. Andrieux, H. Gampp, J. M. Savéant, *Inorg. Chem.* **1986**, *25*, 1778.

[10] a) S. Flandrois, D. Chasseau, *Acta Crystallogr. Sect. B* **1977**, *33*, 2744; b) T. J. Kistenmacher, T. J. Emge, A. N. Bloch, D. O. Cowan, *Acta Crystallogr. Sect. B* **1982**, *38*, 1193.

[11] a) M. F. Bailey, I. E. Maxwell, *J. Chem. Soc. Dalton Trans.* **1972**, 938; b) H. Endres, H. J. Keller, W. Moroni, D. Nöthe, V. Dong, *Acta Crystallogr. Sect. B* **1978**, *34*, 1703.

[12] a) R. Bozio, A. Girlando, C. Pecile, *J. Chem. Soc. Faraday Trans.* **1975**, *71*, 1237; b) F. Bigoli, P. Deplano, F. A. Devillanova, A. Girlando, V. Lippolis, M. L. Mercuri, M. A. Pellinghelli, E. F. Trogu, *J. Mater. Chem.* **1998**, *8*, 1145.

[13] a) E. Kampar, O. Neilands, *Russ. Chem. Rev.* **1986**, *55*, 334; b) A. Painelli, A. Girlando, C. Pecile, *Mol. Cryst. Liq. Cryst.* **1986**, *134*, 1.

[14] a) M. Inoue, M. B. Inoue, *J. Chem. Soc. Faraday Trans.* **1985**, *81*, 539; b) E. Ghezzal, A. Brau, J. P. Farges, P. Dupuis, *Mol. Cryst. Liq. Cryst.* **1992**, *211*, 327.

[15] J. B. Torrance, *Acc. Chem. Res.* **1979**, *12*, 79.

[16] L. Sacconi, F. Mani, A. Bencini in *Comprehensive Coordination Chemistry*, *Vol. 5* (Eds.: G Wilkinson, R. D. Gillard, J. A. McCleverty), Pergamon, Oxford, **1987**, p. 55.

[17] B. J. Hathaway, D. E. Billing, *Coord. Chem. Rev.* **1970**, *5*, 143.

[18] S. Z. Goldberg, R. Eisenber, J. S. Miller, J. A. Epstein, *J. Am. Chem. Soc.* **1976**, *98*, 5173, and references therein.

[19] See, for example O. Kahn, *Molecular Magnetism*, VCH, New York, **1993**, p. 17.

[20] J. W. Hall, W. E. Marsh, R. R. Weller, W. E. Hatfield, *Inorg. Chem.* **1981**, *20*, 1033.

[21] J. Williams, J. R. Ferraro, R. J. Thorn, K. D. Carlson, U. Geiser, H. H. Wang, A. M. Kini, M. H. Whangbo, in *Organic Superconductors. Synthesis, Structure, Properties and Theory* (Ed.: R. N. Grimes), Prentice Hall, Englewood Cliffs, New Jersey, **1992**.

[22] J. Fifani, A. Ramdani, G. Tarragó, *Nouv. J. Chem.* **1977**, *1*, 521.

[23] L. R. Melby, R. J. Herder, W. Mahler, R. E. Benson, W. E. Mochel, *J. Am. Chem. Soc.* **1962**, *84*, 3374.

[24] *International Tables for X-Ray Crystallography*, *Vol. IV*, Kynoch Press, Birmingham, **1974**, p. 72.

[25] G. M. Sheldrichk, SHELX-97, University of Göttingen, Germany, **1997**.